Intestinal glucuronidation protects against chemotherapy-induced toxicity by irinotecan (CPT-11)

Shujuan Chen[a], Mei-Fei Yueh[a], Cyril Bigo[b], Olivier Barbier[b], Kepeng Wang[c], Michael Karin[c,1], Nghia Nguyen[a], and Robert H. Tukey[a,1]

[a]Laboratory of Environmental Toxicology, Departments of Chemistry and Biochemistry and Pharmacology, and [c]Laboratory of Gene Regulation and Signal Transduction, Department of Pharmacology, University of California, San Diego, La Jolla, CA 92023; and [b]Laboratory of Molecular Pharmacology, Centre hospitalier universitaire de Québec Research Center and Faculty of Pharmacy, Laval University, Québec, QC, Canada G1V 4G2

Contributed by Michael Karin, October 11, 2013 (sent for review August 16, 2013)

Camptothecin (CPT)-11 (irinotecan) has been used widely for cancer treatment, particularly metastatic colorectal cancer. However, up to 40% of treated patients suffer from severe late diarrhea, which prevents CPT-11 dose intensification and efficacy. CPT-11 is a prodrug that is hydrolyzed by hepatic and intestinal carboxylesterase to form SN-38, which in turn is detoxified primarily through UDP-glucuronosyltransferase 1A1 (UGT1A1)-catalyzed glucuronidation. To better understand the mechanism associated with toxicity, we generated tissue-specific *Ugt1* locus conditional knockout mouse models and examined the role of glucuronidation in protecting against irinotecan-induced toxicity. We targeted the deletion of the *Ugt1* locus and the *Ugt1a1* gene specifically in the liver ($Ugt1^{\Delta Hep}$) and the intestine ($Ugt1^{\Delta GI}$). Control ($Ugt1^{F/F}$), $Ugt1^{\Delta Hep}$, and $Ugt1^{\Delta GI}$ adult male mice were treated with different concentrations of CPT-11 daily for four consecutive days. Toxicities were evaluated with regard to tissue glucuronidation potential. CPT-11–treated $Ugt1^{\Delta Hep}$ mice showed a similar lethality rate to the CPT-11–treated $Ugt1^{F/F}$ mice. However, $Ugt1^{\Delta GI}$ mice were highly susceptible to CPT-11–induced diarrhea, developing severe and lethal mucositis at much lower CPT-11 doses, a result of the proliferative cell loss and inflammation in the intestinal tract. Comparative expression levels of UGT1A1 in intestinal tumors and normal surrounding tissue are dramatically different, providing for the opportunity to improve therapy by differential gene regulation. Intestinal expression of the UGT1A proteins is critical toward the detoxification of SN-38, whereas induction of the *UGT1A1* gene may serve to limit toxicity and improve the efficacy associated with CPT-11 treatment.

Colorectal cancer (CRC) is the third most commonly diagnosed cancer in the world (1, 2). Camptothecin (CPT)-11 (irinotecan) has been used alone or in combination with other drugs as the first-line therapeutic agent for metastatic CRC (3–5). However, its efficacy and safety are compromised because of severe late diarrhea, the side-effect resulting from CPT-11 bioactivation and subsequent metabolism, generally occurring more than 24 h after the administration of irinotecan (6–9). CPT-11 is a prodrug that is hydrolyzed by carboxylesterase (CES) activity to the active topoisomerase 1 inhibitor, SN-38 (10, 11). Inactivation and detoxification occur primarily by hepatic UDP-glucuronosyltransferase 1A1 (UGT1A1)-catalyzed glucuronidation to form the SN-38 glucuronide (SN-38G), which subsequently undergoes biliary excretion. In 2005 and 2010, the US Food and Drug Administration (FDA) updated the label for CPT-11 regarding the heightened risk of serious side effects for patients with the homozygous and heterozygous *UGT1A1*28* allele (12, 13), recommending an initial dose reduction. Patients who carry the homozygous *UGT1A1*28* alleles, identified as Gilbert's syndrome, have reduced hepatic UGT1A1 expression (14, 15). However, the FDA's recommendation has been questioned because Gilbert's patients receiving CPT-11 therapy have been shown to experience toxicity to a lesser degree than previously anticipated (16, 17). After its excretion into the bile, SN-38G reaches the gastrointestinal tract, where it is subjected to bacterial β-glucuronidase β-linkage cleavage that produces a free SN-38 aglycone (18–21). Recent findings, using specific bacterial β-glucuronidase inhibitors to protect mice from CPT-11–induced late diarrhea, strongly suggest that the enterohepatic circulation of SN-38 plays an essential role in the delayed diarrhea (18, 22). Thus, glucuronidation of SN-38 both in the liver and the GI tract is not a simple detoxification reaction but a rather complex enzymatic process that is closely associated with drug detoxification, toxicity, and efficacy.

Conventionally, the liver is considered the major organ for CPT-11 metabolism, abundantly expressing both CES and UGT enzymes. However, the intestinal tissue from both humans and rodents is also rich in these enzymes (10, 11, 23–25). The direct conversion of CPT-11 to SN-38 in the intestine is considered to be one of the mechanisms leading to intestinal toxicity (10, 26, 27). Alternatively, intestinal microflora-derived β-glucuronidase is capable of catalyzing SN-38G to generate free SN-38 through enterohepatic circulation (18). Thus, we are hypothesizing that levels of intestinal UGT1A activity play a key role in the metabolism of SN-38- and CPT-11–induced intestinal toxicity. Through the generation of tissue-specific *Ugt1* locus conditional knockout animal models, we have directly examined the impact of tissue-specific UGT1A expression toward CPT-11–induced intestinal damage and clearance.

Results

Characterization and Validation of the *Ugt1* Conditional Knockout Mouse Models. Previously we reported the generation of a lethal *Ugt1* knockout mouse model ($Ugt1^{-/-}$) that developed neonatal hyperbilirubinemia with average unconjugated bilirubin levels that exceeded 15 mg/dL (28). $Ugt1^{\Delta Hep}$ mice were

Significance

Camptothecin (CPT)-11 (irinotecan) is an antitumor agent used in cancer chemotherapy primarily for the treatment of solid tumors. CPT-11 is a prodrug that is metabolized by carboxylesterases to the DNA topoisomerase 1 inhibitor, called SN-38. Detoxification of SN-38 occurs by UDP-glucuronosyltransferase 1A1 (UGT1A1)-dependent glucuronidation. A serious side effect of CPT-11 chemotherapy is SN-38–induced intestinal toxicity, which is believed to result in part from the delivery of SN-38 into intestinal tissue through enterohepatic circulation. By selectively targeting the deletion of the *Ugt1* locus in either liver or intestinal tissue, we have confirmed that intestinal UGT1A-specific glucuronidation of SN-38 is essential in preventing SN-38–induced toxicity. Being able to induce intestinal UGT1A1 may be effective in reducing CPT-11 toxicity.

Author contributions: S.C., O.B., M.K., and R.H.T. designed research; S.C., M.-F.Y., C.B., K.W., and N.N. performed research; and S.C., M.-F.Y., and R.H.T. wrote the paper.

The authors declare no conflict of interest.

[1]To whom correspondence may be addressed. E-mail: karinoffice@ucsd.edu or rtukey@ucsd.edu.

This article contains supporting information online at www.pnas.org/lookup/suppl/doi:10.1073/pnas.1319123110/-/DCSupplemental.

achieved by breeding *albumin-Cre* into $Ugt1^{F/F}$ mice (Fig. 1*A*). $Ugt1^{\Delta Hep}$ mice have total serum bilirubin (TSB) levels in the 2–3 mg/dL range shortly after birth and remain at this level during adulthood (Fig. 1*B*). Other than mild hyperbilirubinemia, $Ugt1^{\Delta Hep}$ mice showed no visible abnormalities and matured to adulthood. The deletion of the *Ugt1* locus in liver tissue from $Ugt1^{\Delta Hep}$ neonates resulted in no detectable hepatic UGT1A mRNA and no UGT1A protein expression (Fig. 1 *C* and *D*). Mouse liver microsomes prepared from $Ugt1^{\Delta Hep}$ mice were absent of any detectable bilirubin UGT activity (Fig. 1*E*), further confirming that the *Ugt1* locus was silent in liver tissue of $Ugt1^{\Delta Hep}$ mice. The dramatic difference in TSB accumulation as noted between $Ugt1^{-/-}$ and $Ugt1^{\Delta Hep}$ mice (15 mg/dL vs. 2 mg/dL) implicates an important role for extrahepatic UGT1A1 toward bilirubin glucuronidation and the onset of developmental hyperbilirubinemia.

Deletion of the *Ugt1* locus specifically in intestinal enterocytes ($Ugt1^{\Delta GI}$ mice) was achieved by breeding *villin-Cre* transgenic mice with $Ugt1^{F/F}$ mice (Fig. 2*A*). $Ugt1^{\Delta GI}$ mice showed no abnormality: their TSB levels were similar to those of $Ugt1^{F/F}$ mice (Fig. 2*B*). The intestinal specific deletion of the *Ugt1* locus in $Ugt1^{\Delta GI}$ mice was validated by undetectable intestinal UGT1A1 mRNA expression (Fig. 2*C*), along with nonexistent protein expression as shown in immunoblot analysis (Fig. 2*D*). In addition, bilirubin UGT activity was completely abolished in mouse intestinal microsomes (MIMs) prepared from $Ugt1^{\Delta GI}$ mice (Fig. 2*E*).

The metabolism of SN-38 and bilirubin follows parallel metabolic pathways (29–31). Thus, it is reasonable to speculate that the deletion of the *Ugt1* locus alters the enzymatic activities toward SN-38. By using mouse liver microsomes (MLMs) prepared from $Ugt1^{\Delta Hep}$ adult mice and MIMs from $Ugt1^{\Delta GI}$ adult mice, we examined the UGT activity of SN-38 (Figs. 1*F* and 2*F*). There is a near-complete absence of SN-38 UGT activity in microsomes from $Ugt1^{\Delta Hep}$ and $Ugt1^{\Delta GI}$ mice. It is noticeable that SN-38 UGT activity is more prominent in $Ugt1^{F/F}$ MIMs than in MLMs. Thus, UGT1A specific intestinal glucuronidation may potentially play a key role in protecting the intestinal epithelial cells (IECs) from SN-38–induced toxicity.

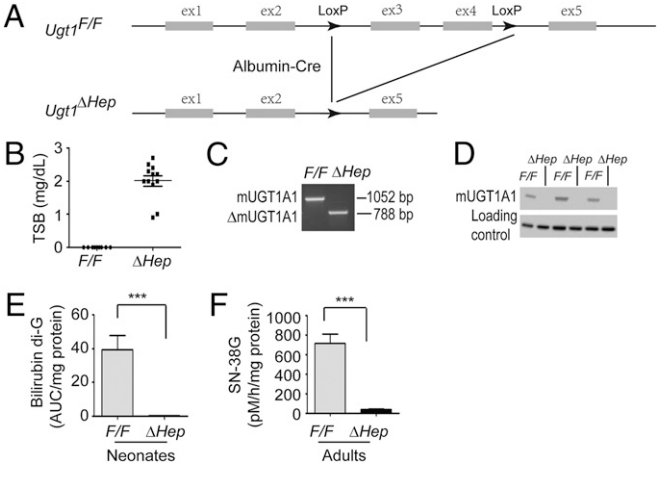

Fig. 1. Liver hepatocyte specific deletion of the *Ugt1a1* gene and its impact on bilirubin and SN-38 glucuronidation. (*A*) The location of the *LoxP* sequence ($Ugt1^{F/F}$) and the result of albumin-Cre–mediated deletion ($Ugt1^{\Delta Hep}$ mice). (*B*) $Ugt1^{\Delta Hep}$ mice accumulate 2–3 mg/dL TSB. (*C*) In the $Ugt1^{\Delta Hep}$ liver, exons 3 and 4 are deleted in liver tissue as shown by RT-PCR analysis. Primers used are specific for exons 1 and 5. (*D*) Western blot analysis shows no expression of UGT1A1 in $Ugt1^{\Delta Hep}$ MLMs. (*E*) Bilirubin glucuronidation analysis was performed in neonatal $Ugt1^{\Delta Hep}$ MLMs (mean ± SEM). (*F*) SN-38 glucuronidation analysis was performed by using adult $Ugt1^{\Delta Hep}$ MLMs (mean ± SEM). ***$P < 0.001$, Student *t* test.

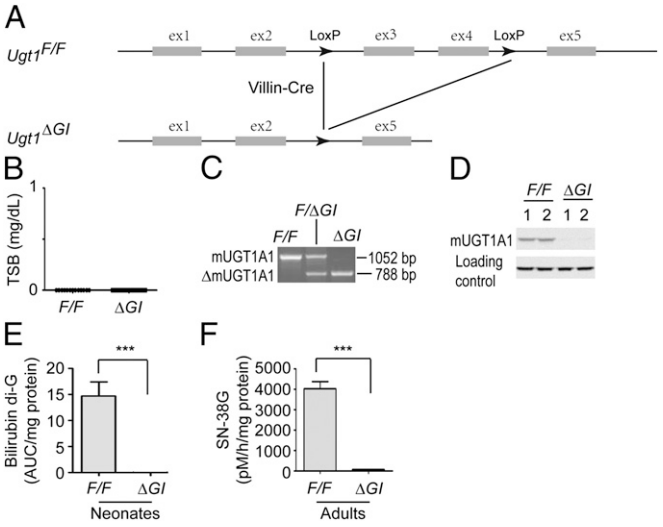

Fig. 2. Intestinal enterocyte-specific deletion of the *Ugt1a1* gene and its impact on bilirubin and SN-38 glucuronidation. (*A*) The generation of villin-Cre–mediated deletion ($Ugt1^{\Delta GI}$ mice). (*B*) $Ugt1^{\Delta GI}$ mice have normal or undetectable levels of TSB. (*C*) In the intestines of $Ugt1^{\Delta GI}$ mice, exons 3 and 4 are deleted, as shown by RT-PCR analysis. (*D*) Western blot analysis shows no expression of UGT1A1 protein in $Ugt1^{\Delta GI}$ MIMs. (*E*) Bilirubin glucuronidation assay was conducted in neonatal $Ugt1^{\Delta GI}$ MIMs (mean ± SEM). (*F*) SN-38 glucuronidation activity in adult $Ugt1^{\Delta GI}$ MIMs (mean ± SEM). ***$P < 0.001$, Student *t* test.

Survival Rate. After mice were treated with CPT-11 after the 4-d dosing plan, CPT-11–induced lethality was determined over the course of 3 wk. GraphPad Prism Statistics software was used to generate the survival vs. time curves, and *P* values were calculated by comparing the entire survival curves. Conventionally, liver is considered the major organ for CPT-11 metabolism and SN-38 detoxification. Because SN-38 is detoxified through UGT1A-catalyzed glucuronidation, we anticipated that a higher level of SN-38 toxicities would be observed in $Ugt1^{\Delta Hep}$ mice as a result of hepatic UGT1A deletion. Unexpectedly, when mice were treated with CPT-11 at a 100-mg/kg dosage, the survival rate of $Ugt1^{\Delta Hep}$ mice was ∼25%, which was similar to the survival rate of $Ugt1^{F/F}$ mice (Fig. 3*A*). When we adjusted CPT-11 dosage to 75 mg/kg, a similar survival rate (∼50%) was observed in both $Ugt1^{F/F}$ and $Ugt1^{\Delta Hep}$ mice (Fig. 3*B*). This result suggested that hepatic UGT1A enzyme activity may not be predominantly responsible for the CPT-11 detoxification. To our surprise, $Ugt1^{\Delta GI}$ mice with intestinal deletion of the *Ugt1* locus were extremely sensitive in response to CPT-11 treatment. After i.p. injection of CPT-11 at 50 mg/kg for 4 consecutive days, all $Ugt1^{\Delta GI}$ mice died at day 6, in comparison with $Ugt1^{F/F}$ mice with the survival rate of ∼60% (Fig. 3*C*). When mice were treated with CPT-11 at a 25-mg/kg dosage, none of the $Ugt1^{\Delta GI}$ mice survived, in contrast to a 100% survival rate in $Ugt1^{F/F}$ mice (Fig. 3*D*). When the CPT-11 dosage was further lowered to 10 mg/kg, 2 of 10 $Ugt1^{\Delta GI}$ mice died, and all $Ugt1^{F/F}$ mice survived (Fig. 3*E*). These results suggested that intestinal UGT1A enzymes play a pivotal role in protecting mice from CPT-11–induced toxicities.

Weight Loss. The kinetics of CPT-11–induced body weight loss was determined over the course of 2 wk. Weight loss was evidenced in both $Ugt1^{F/F}$ and $Ugt1^{\Delta Hep}$ mice as early as 24 h after the first administration of CPT-11 at 75 mg/kg and reached 25–35% loss by day 8, 4 d after the last dose of CPT-11 (Fig. 4*A*). For the surviving mice, their weights started to return to the normal range in 2 wk (Fig. 4*A*). No significant difference in weight loss was observed between $Ugt1^{\Delta Hep}$ and control $Ugt1^{F/F}$ mice ($P >$

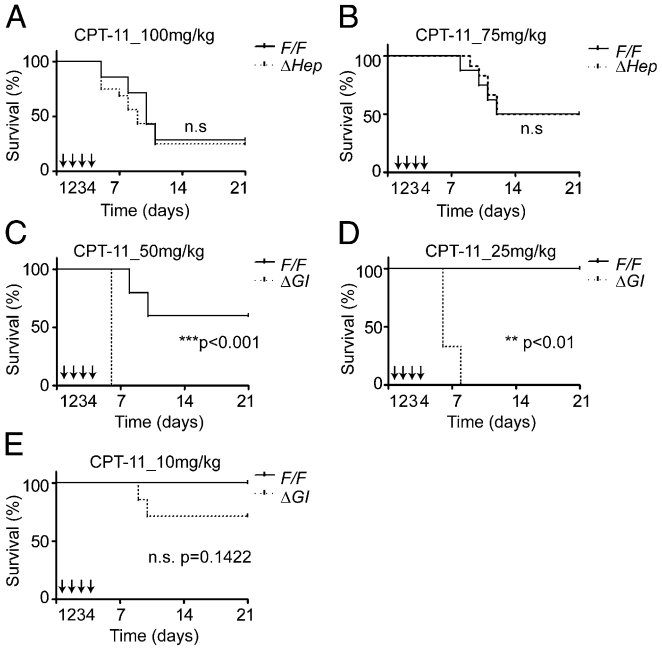

Fig. 3. CPT-11–induced lethality in $Ugt1^{F/F}$ vs. $Ugt1^{\Delta Hep}$ mice (*A* and *B*) and $Ugt1^{F/F}$ vs. $Ugt1^{\Delta GI}$ mice (*C*–*E*). Age-matched adult male mice or littermates were used for these experiments. CPT-11 was administered to $Ugt1^{F/F}$, $Ugt1^{\Delta Hep}$, and $Ugt1^{\Delta GI}$ mice (10 mice per group) once per day for 4 constitutive days by i.p. injection. The respective doses are indicated above each graph. CPT-11–induced lethality was determined over the course of 3 wk. GraphPad Prism software was used to graph the survival vs. time curves and to calculate the *P* value.

0.05, two-way ANOVA). In contrast, the weight loss in $Ugt1^{F/F}$ and $Ugt1^{\Delta GI}$ mice in response to CPT-11 treatment was significantly different. After CPT-11 treatment at 10 mg/kg, no obvious weight loss (less than 5%) was observed in $Ugt1^{F/F}$ mice; by comparison, weight loss as high as 35–40% was seen in $Ugt1^{\Delta GI}$ mice at day 8. The weight loss between $Ugt1^{\Delta GI}$ and $Ugt1^{F/F}$ mice was statistically significant ($^{****}P < 0.0001$, two-way ANOVA), as demonstrated in Fig. 4*B*. In $Ugt1^{\Delta GI}$ mice, the weight loss was conversely correlated to the survival rate in response to CPT-11 treatment. Mice with weight loss less than 25% tended to have the ability to reverse damage; they eventually survived and returned to their normal weight in 2 wk, as shown in Fig. 4*C*. However, mice with weight loss greater than 25% often resulted in lethality; ~93.8% of these mice died. The association between weight loss and survival is considered to be extremely statistically significant, as demonstrated in the contingency table in Fig. 4*C*. The two-tailed *P* value was calculated through Fisher's exact test.

Histological Analysis of Intestinal Tissue After CPT-11 Treatment. $Ugt1^{F/F}$ and $Ugt1^{\Delta GI}$ mice were treated with either control or CPT-11 at 10 mg/kg for 4 d and were killed on day 5 after the initial dose. Duodenum, jejunum, ileum, and colon samples were dissected, and each of the sections was split longitudinally into two halves. Half of the tissues were either frozen immediately in optimal cutting temperature (OCT) compound or fixed in 10% (vol/vol) buffered formalin for 24 h and transferred to 70% (vol/vol) ethanol for subsequent paraffin embedding and histological analysis, and the other half of the tissue samples were snap frozen in liquid nitrogen for RNA preparation. Histological examination was performed on paraffin-embedded sections after H&E staining. Immunohistochemical analyses were performed with the use of antiproliferating cell antigen (anti-Ki67 antibody) to assay proliferation.

The histological examination indicated that all tissue samples from CPT-11–treated $Ugt1^{\Delta GI}$ mice demonstrated moderate to severe damage, as shown in Fig. 5. Tightly arrayed epithelial cells were displayed in the control samples, whereas obvious short villi and crypt loss were observed in duodenum, jejunum, and ileum in moderately damaged intestines. With the severely damaged intestines, the intestinal morphology and integrity were severely disrupted, with complete abolishment of the top villi along with severe inflammation (Fig. 5). In comparison with the damage in small intestine, the morphology of colon tissues in CPT-11–treated mice showed fewer changes; however, obvious hyperplasia of goblet cells was observed in colon tissues of CPT-11–treated $Ugt1^{\Delta GI}$ mice (Fig. 5).

CPT-11–induced intestinal toxicity was further studied by immunofluorescence staining of the proliferative marker Ki67 (Fig. 6*A*). In CPT-11–treated $Ugt1^{F/F}$ mice, the layer of the proliferative cells remained almost intact in the intestinal tract (Fig. 6 *A* and *B*). In contrast, severe proliferative cell loss was observed in CPT-11–treated $Ugt1^{\Delta GI}$ mice, implying a difficult recovery from the damage, in accordance with the slow weight recovery of $Ugt1^{\Delta GI}$ mice as demonstrated in Fig. 4*B*. In addition, very few Ki67-positive cells were detected in the severely damaged group (Fig. 6*A*). Mice with severely damaged intestines are closely correlated with those with severe weight loss (greater than 25% loss of their original weight). The inability to proliferate in the severely damaged intestines of $Ugt1^{\Delta GI}$ mice after CPT-11 treatment could be the root cause of the lethality. The loss of Ki67-positive cells in colon tissue as a result of CPT-11 treatment was less severe compared with the damage in the small intestine sections (Fig. 6*B*).

Filtration and inflammation were also observed in the histological studies in both small intestine and colon tissues after mice were treated with CPT-11. IL-6, a multifunctional cytokine that acts on IECs (32), was used as an inflammatory biomarker for CPT-11–induced intestinal damage. Total RNA was prepared from the different sections and used to quantitate the expression of IL-6 by RT and quantitative PCR (qPCR). Results in Fig. 6 *C* and *D* demonstrated that in both small intestine and colon, IL-6 was dramatically increased in $Ugt1^{\Delta GI}$ mice in comparison with $Ugt1^{F/F}$ mice after CPT-11 treatment.

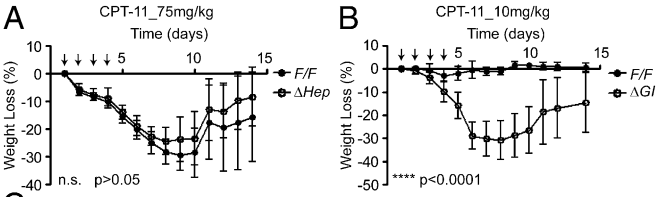

C

Weight Loss	Survival	Death	Total
< 25%	12	0	12
> 25%	2	30	32
Total	14	30	44

Fig. 4. CPT-11–induced weight loss and hematotoxicity in $Ugt1^{F/F}$, $Ugt1^{\Delta Hep}$, and $Ugt1^{\Delta GI}$ mice. Age-matched adult male mice or littermates were used for these experiments. (*A*) CPT-11 was administered to $Ugt1^{F/F}$ and $Ugt1^{\Delta Hep}$ mice (10 mice per group) at the 75-mg/kg dose once per day for 4 constitutive days by i.p. injection. Weight was monitored daily. After data collection, percentage of weight loss in comparison with the pretreatment was described as the mean ± SD. Two-way ANOVA was used for statistical analysis. (*B*) Percentage of weight loss in $Ugt1^{F/F}$ and $Ugt1^{\Delta GI}$ mice after CPT-11 treatment at 10 mg/kg after the same dosing regimen as described. (*C*) Correlation of survival and weight loss. Data are described in a 2 × 2 contingency table. Two-tailed *P* value was analyzed by Fisher's exact test.

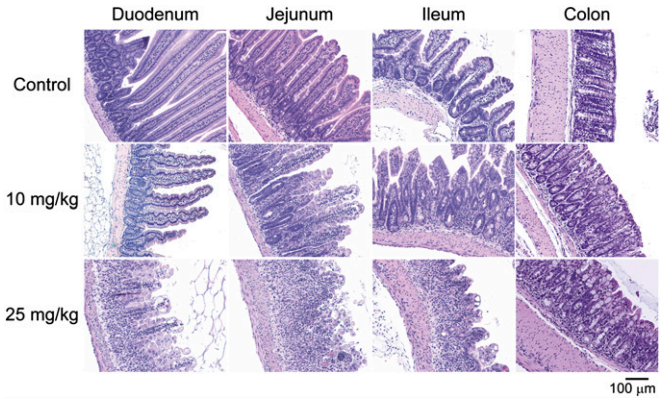

Fig. 5. CPT-11–induced intestinal damage in $Ugt1^{\Delta GI}$ mice. Intestinal tissue from untreated (Control) or treated $Ugt1^{\Delta GI}$ mice was analyzed on the fifth day after 4 consecutive days of treatment with 10 or 25 mg/kg CPT-11. Intestinal tissue was sectioned into duodenum, jejunum, ileum, and colon and the morphology of the intestines photographed after H&E staining.

Hematological Evaluation. Neutropenia and leukopenia are known clinical side effects of CPT-11 treatment. In this study, murine whole EDTA blood samples were collected before and after the CPT-11 treatment. Samples were analyzed for white blood counts with leukocyte differential on a Hemavet 850FS Multi Species Hematology System. As expected, white blood counts decreased significantly in mice after CPT-11 exposure. Similar results were observed with the leukocyte counts. However, neither $Ugt1^{\Delta Hep}$ mice nor $Ugt1^{\Delta GI}$ mice showed more severe hematological toxicities than control $Ugt1^{F/F}$ mice (Fig. S1).

Altered Gene Expression in Colorectal Tumors. Expression of the *Ugt1* locus in the gastrointestinal tract protects tissue from the toxic actions of CPT-11 treatment. However, CRC has been linked to the onset of inflammation (33), an event that is associated with a reduction in drug metabolism. To define the impact of cancer on gene regulation in both healthy and tumor tissue, we examined $Apc^{F/wt}$ mice that harbored a *Cdx2-Cre* transgene (CPC-APC mice) in which colorectal tumorigenesis was driven by *Apc* allelic loss (34). Both tumor tissues and the adjacent normal colon tissues were collected, and RNA was prepared for qPCR analysis. Results show that genes associated with the *Ugt1* locus in tumor tissue were reduced to less than 10% in comparison with the surrounding normal tissue (Fig. 7). Along with *Ugt1a1*, *Ces1* and *Ces2* gene expression were also dramatically lower than in surrounding normal tissue. Other genes important in drug metabolism, such as *Cyp3a11* and *Cyp4a10*, also displayed dramatic reduction in gene expression. However, other *Cyp* genes were up-regulated along with selective efflux transporter genes *Mrp1* and *Mrp2*. Because expression of many of the genes associated with drug metabolism have been linked to control by xenobiotic nuclear receptors (XNRs), it was not a surprise to see reduced expression of *Pxr*, *Car*, and *Lxrα* gene expression. The relationship between XNR expression and target gene expression is not entirely correlated, because the CAR target gene *Cyp2b10* is robustly induced in tumor tissue. In general, these findings indicate that up-regulation of *Mrp1* and *Mrp2* gene expression and reduction in *Ces1/2* activity could lead to drug resistance, whereas down-regulation of XNRs along with *Ugt1a1* would sensitize the tumor toward SN-38 exposure.

Discussion

Patients treated with CPT-11 suffer from severe late diarrhea, which prevents CPT-11 dose intensification and compromises efficacy. The exact mechanism of CPT-11–induced late diarrhea is unknown, but IEC damage resulting from exposure to high concentrations of the active metabolite SN-38 is considered the initial step of the toxicity. Inactivation and detoxification occurs primarily by UGT1A-catalyzed glucuronidation to form the SN-38 glucuronide, which subsequently undergoes biliary excretion. Given the fact that hepatocytes are rich in UGT1A1 protein and are responsible for the transport of SN-38G into the bile, liver is conventionally considered as the most important organ for irinotecan detoxification. In this study we used the Cre-recombinase strategy for targeted gene deletion, through which we have generated *Ugt1* locus conditional knockout mice that targeted deletion of the *Ugt1* locus specifically in liver tissue ($Ugt1^{\Delta Hep}$ mice) and the intestinal tract ($Ugt1^{\Delta GI}$ mice).

The results show in the complete absence of the hepatic *Ugt1* locus and UGT1A proteins, $Ugt1^{\Delta Hep}$ mice are resistant toward CPT-11 treatment at the dose tested and, therefore, maintain integrity of the intestinal tract. Conversely, mice with intestinal-specific deletion of the *Ugt1* locus ($Ugt1^{\Delta GI}$) are extremely sensitive to CPT-11 exposure; severe weight loss was observed as a result of bloody diarrhea, which eventually leads to animal death. The results clearly demonstrate that extrahepatic instead of hepatic expression of the UGT1A proteins is more critical to the detoxification of SN-38. Consistent with these studies, the importance of intestinal enzymes in CPT-11 toxicity has also been suggested in tissue-specific profiling studies of CES. Human intestinal CES2 exhibits a higher affinity and velocity than human hepatic CES1, demonstrating the significant ability to hydrolyze CPT-11 (10, 26, 27). Intestinal selective CES inhibitors have been suggested as a new clinical target to minimize CPT-11–induced late diarrhea (35, 36). However, we note that *Ces1/2* gene expression is already greatly reduced in tumor tissue, indicating that further reduction in activity would minimize therapeutic efficacy.

Through enterohepatic circulation, free SN-38 conversion from SN-38G catalyzed by bacterial β-glucuronidase present in intestinal microflora (Fig. S2) is also considered to be an additional mechanism that is related to CPT-11 toxicity (18). By using specific bacterial β-glucuronidase inhibitors to protect mice from CPT-11–induced late diarrhea, recent findings strongly suggest that enterohepatic circulation of SN-38 plays an essential role in delayed

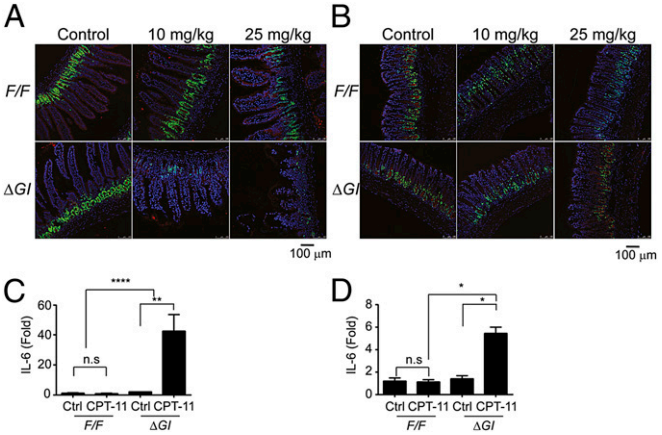

Fig. 6. (*A*) Intestinal epithelium cell proliferation resulting from CPT-11 treatment. $Ugt1^{F/F}$ and $Ugt1^{\Delta GI}$ mice were treated with 10 or 25 mg/kg CPT-11 as outlined and cellular proliferation monitored by Ki67 (in green) and β-catenin (in red) immunohistochemistry for cell membrane staining, along with DAPI nuclear counterstain (blue). (*B*) Ki67, β-catenin, and DAPI immunofluorescences staining in colon tissues. (*C*) After treatment with irinotecan at 10 mg/kg, on day 5, jejunum total RNA was prepared from the $Ugt1^{F/F}$ and $Ugt1^{\Delta GI}$ mice and used to quantitate the expression of cytokines IL-6 by RT and qPCR. (*D*) IL-6 expression was also determined in colon tissues from the CPT-11 treated $Ugt1^{F/F}$ and $Ugt1^{\Delta GI}$ mice. Results were described as mean ± SEM. $*P < 0.05$, $**P < 0.01$, $****P < 0.0001$, Student *t* test.

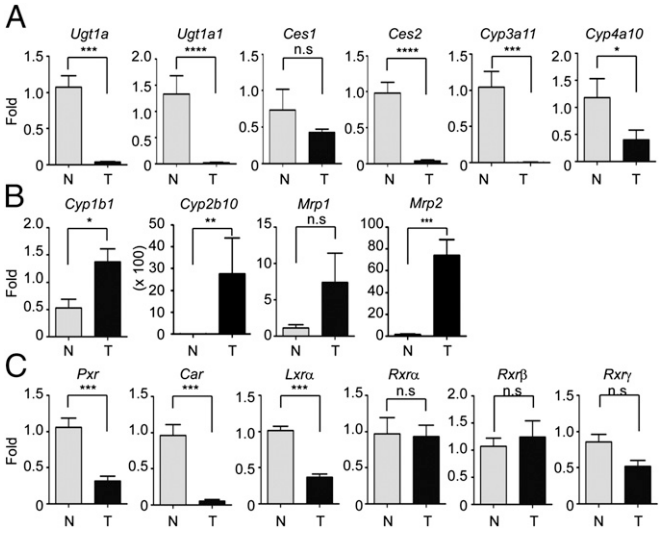

Fig. 7. Gene expression patterns in normal tissue (N) and colon tumors (T). Both tumor tissues and the adjacent normal colon tissues were collected from CPC-APC mice, total RNA prepared, and gene expression monitored by RT followed by qPCR analysis. Each gene analysis was performed on five individual samples (mean ± SEM). $*P < 0.05$, $**P < 0.01$, $***P < 0.001$, Student *t* test. Gene expression is either repressed (*A*) or induced (*B*) in tumor tissue. (*C*) Xenobiotic nuclear receptor expression patterns.

diarrhea (18, 22). After release from its glucuronide form, free SN-38 is reabsorbed into the luminal side of IECs. It is likely that intestinal UGT1A proteins catalyze the glucuronidation of SN-38, which protects the IECs from excessive exposure to the free SN-38. Conversely, in the absence of intestinal UGT1A proteins and UGT1A-mediated glucuronidation activity, IECs are exposed directly to free SN-38 that leads to a higher degree of toxicity. It is worth noting that although β-glucuronidase inhibitors protect mice from CPT-11-induced toxicity, these inhibitors block the enterohepatic circulation of SN-38 by facilitating its clearance from the body. Through this process, IECs are protected from free SN-38 exposure. Because the colon is the target tissue for CRC therapy, lower concentrations of active SN-38 in the colon may also contribute to the decreasing chemotherapeutic efficacy of CPT-11.

As we propose in Fig. S2, induction and regulation of the intestinal *UGT1A* genes in healthy tissue may provide an effective approach toward balancing CPT-11 toxicity and efficacy. In colon cancer, human *UGT1A* gene suppression has been suggested as a putative early event that occurs in malignant tumors but not in benign tumors (37). Consistent with previous findings, our results demonstrate that the *Ugt1a1* gene (and the *Ugt1a* genes) in mice is down-regulated in colon tumor tissue and expressed normally in the adjacent healthy tissue. It is currently unknown why gene expression is dramatically altered in tumor tissue. The decrease in *Ugt1a* gene expression in colon cancer tissue may result from epigenetic modulation, inhibition by inflammatory factors, or attenuation in XNR nuclear localization (38). If tumor *Ugt1a* gene expression is impaired, induction of gene activity in nondiseased normal tissue may protect the surrounding epithelial cells from SN-38 damage by increasing glucuronidation capacity and improving drug tolerance. For example, UGT1A1, the primary UGT involved in SN-38 glucuronidation (15), can be regulated by induction of the human *UGT1A1* gene after activation of XNRs PXR (39, 40), CAR (15), and PPARα (41). One could envision that potential therapeutics could be developed to target induction of the *UGT1A1* gene in healthy tissue, thus providing an added level of protection toward the toxicity inherent in the accumulation of SN-38.

In conclusion, intestinal expression of the UGT1A proteins is critical toward the detoxification of SN-38. Regulation of intestinal UGT1A1 may serve as a therapeutic target for improving the therapeutic index and efficacy associated with CPT-11 chemotherapeutic treatment.

Materials and Methods

Generation of *Ugt1* Conditional Knockout Mouse Models. The Cre/loxP recombination system was used for the generation of cell type-specific gene targeting for the mouse *Ugt1* locus (42–45). When *Ugt1a1* intron 2 floxed/intron 4 floxed ($Ugt1^{F/F}$) mice were bred with *albumin-Cre* or *villin-Cre* mice, Cre-mediated recombination resulted in deletion of exons 3 and 4 specifically in either liver hepatocytes ($Ugt1^{\Delta Hep}$ mice) or intestinal enterocytes ($Ugt1^{\Delta GI}$ mice). Because exons 3 and 4 of the *Ugt1a1* gene are common exons for the other *Ugt1a* genes (28), the entire *Ugt1* locus is rendered inactive in a tissue-specific fashion.

Animal Treatment with CPT-11. CPT-11 was supplied in 5-mL vials that contain 100 mg of irinotecan hydrochloride (20 mg/mL) under the trade name Camptosar ready-to-use solution by Pfizer. All mouse experiments and procedures are in accordance with the Guide for the Care and Use of Laboratory Animals and were approved by the University of California, San Diego Animal Care Committee. CPT-11 was administered to mice once per day for 4 constitutive days by i.p. injection. Ten age-matched male mice (from two to three littermates) per group were used for experiments to achieve statistical significance. GraphPad Prism softward was used for graphing and data statistics.

Histological Analysis. Mice were killed, and duodenum, jejunum, ileum, and colon samples were dissected. Tissues were fixed for subsequent paraffin embedding. A tissue histological examination was performed on paraffin-embedded sections using 6-μm-thick, 200-μm step serial sections stained with H&E. For immunohistochemical staining, intestinal tissue was embedded into OCT compound in vinyl mold and placed immediately into dry ice/isopentane slurry until the OCT turned white. Cryo-sectioning was carried out at a thickness of 10 μm in a cryostat. Frozen slides were stained with antibodies against Ki67 (GeneTex, GTX16667) and β-catenin (Santa Cruz Biotechnology, sc-1496) for overnight at 4 °C. Slides were then washed and stained with Alexa-488–conjugated donkey anti-rabbit, or Alexa-594–conjugated donkey anti-goat antibodies (Life Technologies), alongside a DAPI counterstaining. Mounted slides were examined under Leica SPE confocal microscopy.

Immunoblotting. MLMs and MIMs were prepared as previously outlined (46). All Western blots were performed by using NuPAGE BisTris-polyacrylamide gels as outlined by the supplier (Invitrogen). Membranes were washed and exposed to horseradish peroxidase-conjugated secondary antibodies for 1 h at room temperature. Protein was detected by the ECL Plus Western blotting detection system (Amersham Biosciences) and was visualized by the BioRad gel documentation system.

Total RNA Preparation and RNA Analysis by RT-PCR and qPCR. Approximately 100 mg of tissues was homogenized in 1 mL TRIzol (Invitrogen) (40). Using iScript Reverse Transcriptase (BioRad), 1 μg of total RNA was used for the generation of cDNA in a total volume of 20 μL as outlined by the manufacturer. After synthesis of cDNA, 1 μL was used for PCR reactions or in real-time PCRs conducted with a Ssoadvanced SYBR Green Supermix (BioRad) using a CFX96 Touch Real-Time PCR detection system (BioRad). *Ct* values of gene interested were normalized to those of the mouse cyclophilin gene (ΔCt) and were expressed as induction fold over controls using the equation = $2^{-(\Delta Ct\text{Sample} - \Delta Ct\text{Control})}$. Primer sequences are listed in Table S1.

Bilirubin and SN-38 Glucuronidation Assays. Bilirubin glucuronidation activity and SN-38 glucuronidation assays were performed at 37 °C as described previously (47, 48). Bilirubin di-glucuronide and SN-38 glucuronide formation was determined by liquid chromatography (Alliance 2695) coupled to tandem mass spectrometry (API 4000, Applied Biosystems). The HPLC system used was equipped with a 50 × 3.2-mm Columbus C18 column (Phenomenex).

ACKNOWLEDGMENTS. This work was supported in part by US Public Health Service Grants R21CA171008 (to S.C.), ES010337 (to R.H.T. and M.K.), GM086713 and GM100481 (to R.H.T.), and AI043477 (to M.K.); Canadian Institutes of Health Research Grants MOP-84338 and MSH95330 and Canada Foundation for Innovation Project #17745 (to O.B.); and a Laval University Faculty of Pharmacy fellowship (to C.B.).

1. Rim SH, Seeff L, Ahmed F, King JB, Coughlin SS (2009) Colorectal cancer incidence in the United States, 1999-2004: An updated analysis of data from the National Program of Cancer Registries and the Surveillance, Epidemiology, and End Results Program. *Cancer* 115(9):1967–1976.
2. Weir HK, et al. (2003) Annual report to the nation on the status of cancer, 1975-2000, featuring the uses of surveillance data for cancer prevention and control. *J Natl Cancer Inst* 95(17):1276–1299.
3. Pizzolato JF, Saltz LB (2003) The camptothecins. *Lancet* 361(9376):2235–2242.
4. Pommier Y (2006) Topoisomerase I inhibitors: Camptothecins and beyond. *Nat Rev Cancer* 6(10):789–802.
5. Smith NF, Figg WD, Sparreboom A (2006) Pharmacogenetics of irinotecan metabolism and transport: An update. *Toxicol In Vitro* 20(2):163–175.
6. Rothenberg ML, et al. (1993) Phase I and pharmacokinetic trial of weekly CPT-11. *J Clin Oncol* 11(11):2194–2204.
7. Rowinsky EK, et al. (1994) Phase I and pharmacological study of the novel topoisomerase I inhibitor 7-ethyl-10-[4-(1-piperidino)-1-piperidino]carbonyloxycamptothecin (CPT-11) administered as a ninety-minute infusion every 3 weeks. *Cancer Res* 54(2):427–436.
8. Ma MK, McLeod HL (2003) Lessons learned from the irinotecan metabolic pathway. *Curr Med Chem* 10(1):41–49.
9. Mathijssen RH, et al. (2001) Clinical pharmacokinetics and metabolism of irinotecan (CPT-11). *Clin Cancer Res* 7(8):2182–2194.
10. Hatfield MJ, et al. (2011) Organ-specific carboxylesterase profiling identifies the small intestine and kidney as major contributors of activation of the anticancer prodrug CPT-11. *Biochem Pharmacol* 81(1):24–31.
11. Sanghani SP, et al. (2003) Carboxylesterases expressed in human colon tumor tissue and their role in CPT-11 hydrolysis. *Clin Cancer Res* 9(13):4983–4991.
12. Kim TW, Innocenti F (2007) Insights, challenges, and future directions in irinogenetics. *Ther Drug Monit* 29(3):265–270.
13. Liu CY, et al. (2008) UGT1A1*28 polymorphism predicts irinotecan-induced severe toxicities without affecting treatment outcome and survival in patients with metastatic colorectal carcinoma. *Cancer* 112(9):1932–1940.
14. Fujiwara R, Nguyen N, Chen S, Tukey RH (2010) Developmental hyperbilirubinemia and CNS toxicity in mice humanized with the UDP glucuronosyltransferase 1 (*UGT1*) locus. *Proc Natl Acad Sci USA* 107(11):5024–5029.
15. Cai H, et al. (2010) A humanized *UGT1* mouse model expressing the *UGT1A1*28* allele for assessing drug clearance by UGT1A1-dependent glucuronidation. *Drug Metab Dispos* 38(5):879–886.
16. Toffoli G, et al. (2006) The role of UGT1A1*28 polymorphism in the pharmacodynamics and pharmacokinetics of irinotecan in patients with metastatic colorectal cancer. *J Clin Oncol* 24(19):3061–3068.
17. Palomaki GE, Bradley LA, Douglas MP, Kolor K, Dotson WD (2009) Can UGT1A1 genotyping reduce morbidity and mortality in patients with metastatic colorectal cancer treated with irinotecan? An evidence-based review. *Genet Med* 11(1):21–34.
18. Wallace BD, et al. (2010) Alleviating cancer drug toxicity by inhibiting a bacterial enzyme. *Science* 330(6005):831–835.
19. Tobin P, et al. (2006) The in vitro metabolism of irinotecan (CPT-11) by carboxylesterase and beta-glucuronidase in human colorectal tumours. *Br J Clin Pharmacol* 62(1):122–129.
20. Yamamoto M, et al. (2008) Metabolism of irinotecan and its active metabolite SN-38 by intestinal microflora in rats. *Oncol Rep* 20(4):727–730.
21. Prijovich ZM, Chen KC, Roffler SR (2009) Local enzymatic hydrolysis of an endogenously generated metabolite can enhance CPT-11 anticancer efficacy. *Mol Cancer Ther* 8(4):940–946.
22. Takasuna K, et al. (2006) Optimal antidiarrhea treatment for antitumor agent irinotecan hydrochloride (CPT-11)-induced delayed diarrhea. *Cancer Chemother Pharmacol* 58(4):494–503.
23. Strassburg CP, et al. (2000) Polymorphic gene regulation and interindividual variation of UDP-glucuronosyltransferase activity in human small intestine. *J Biol Chem* 275(46): 36164–36171.
24. Strassburg CP, Nguyen N, Manns MP, Tukey RH (1999) UDP-glucuronosyltransferase activity in human liver and colon. *Gastroenterology* 116(1):149–160.
25. Strassburg CP, Manns MP, Tukey RH (1998) Expression of the *UDP-glucuronosyltransferase 1A* locus in human colon. Identification and characterization of the novel extrahepatic UGT1A8. *J Biol Chem* 273(15):8719–8726.
26. Humerickhouse R, Lohrbach K, Li L, Bosron WF, Dolan ME (2000) Characterization of CPT-11 hydrolysis by human liver carboxylesterase isoforms hCE-1 and hCE-2. *Cancer Res* 60(5):1189–1192.
27. Khanna R, Morton CL, Danks MK, Potter PM (2000) Proficient metabolism of irinotecan by a human intestinal carboxylesterase. *Cancer Res* 60(17):4725–4728.
28. Nguyen N, et al. (2008) Disruption of the ugt1 locus in mice resembles human Crigler-Najjar type I disease. *J Biol Chem* 283(12):7901–7911.
29. Ruggiero A, Coccia P, Scalzone M, Attinà G, Riccardi R (2009) Treatment of childhood sarcoma with irinotecan: Bilirubin level as a predictor of gastrointestinal toxicity. *J Chemother* 21(6):693–697.
30. Iyer L, et al. (1999) Phenotype-genotype correlation of in vitro SN-38 (active metabolite of irinotecan) and bilirubin glucuronidation in human liver tissue with UGT1A1 promoter polymorphism. *Clin Pharmacol Ther* 65(5):576–582.
31. Iyer L, et al. (1998) Genetic predisposition to the metabolism of irinotecan (CPT-11). Role of uridine diphosphate glucuronosyltransferase isoform 1A1 in the glucuronidation of its active metabolite (SN-38) in human liver microsomes. *J Clin Invest* 101(4):847–854.
32. Grivennikov S, et al. (2009) IL-6 and Stat3 are required for survival of intestinal epithelial cells and development of colitis-associated cancer. *Cancer Cell* 15(2):103–113.
33. Grivennikov SI, et al. (2012) Adenoma-linked barrier defects and microbial products drive IL-23/IL-17-mediated tumour growth. *Nature* 491(7423):254–258.
34. Hinoi T, et al. (2007) Mouse model of colonic adenoma-carcinoma progression based on somatic Apc inactivation. *Cancer Res* 67(20):9721–9730.
35. Wadkins RM, et al. (2004) Discovery of novel selective inhibitors of human intestinal carboxylesterase for the amelioration of irinotecan-induced diarrhea: Synthesis, quantitative structure-activity relationship analysis, and biological activity. *Mol Pharmacol* 65(6):1336–1343.
36. Hatfield MJ, et al. (2010) Biochemical and molecular analysis of carboxylesterase-mediated hydrolysis of cocaine and heroin. *Br J Pharmacol* 160(8):1916–1928.
37. Strassburg CP, Manns MP, Tukey RH (1997) Differential down-regulation of the *UDP-glucuronosyltransferase 1A* locus is an early event in human liver and biliary cancer. *Cancer Res* 57(14):2979–2985.
38. Kacevska M, et al. (2011) Extrahepatic cancer suppresses nuclear receptor-regulated drug metabolism. *Clin Cancer Res* 17(10):3170–3180.
39. Xie W, et al. (2003) Control of steroid, heme, and carcinogen metabolism by nuclear pregnane X receptor and constitutive androstane receptor. *Proc Natl Acad Sci USA* 100(7):4150–4155.
40. Chen S, Yueh MF, Evans RM, Tukey RH (2012) Pregnane-x-receptor controls hepatic glucuronidation during pregnancy and neonatal development in humanized UGT1 mice. *Hepatology* 56(2):658–667.
41. Senekeo-Effenberger K, et al. (2007) Expression of the human UGT1 locus in transgenic mice by 4-chloro-6-(2,3-xylidino)-2-pyrimidinylthioacetic acid (WY-14643) and implications on drug metabolism through peroxisome proliferator-activated receptor alpha activation. *Drug Metab Dispos* 35(3):419–427.
42. Kühn R, Torres RM (2002) Cre/loxP recombination system and gene targeting. *Methods Mol Biol* 180:175–204.
43. Ghosh K, Van Duyne GD (2002) Cre-loxP biochemistry. *Methods* 28(3):374–383.
44. Le Y, Sauer B (2000) Conditional gene knockout using cre recombinase. *Methods Mol Biol* 136:477–485.
45. Utomo AR, Nikitin AY, Lee WH (1999) Temporal, spatial, and cell type-specific control of Cre-mediated DNA recombination in transgenic mice. *Nat Biotechnol* 17(11): 1091–1096.
46. Chen S, et al. (2005) Tissue-specific, inducible, and hormonal control of the human UDP-glucuronosyltransferase-1 (*UGT1*) locus. *J Biol Chem* 280(45):37547–37557.
47. Verreault M, et al. (2006) The liver X-receptor alpha controls hepatic expression of the human bile acid-glucuronidating UGT1A3 enzyme in human cells and transgenic mice. *Hepatology* 44(2):368–378.
48. Gagnon JF, Bernard O, Villeneuve L, Têtu B, Guillemette C (2006) Irinotecan inactivation is modulated by epigenetic silencing of UGT1A1 in colon cancer. *Clin Cancer Res* 12(6):1850–1858.